JOURNAL OF PROPULSION AND POWER
Vol. 19, No. 5, September–October 2003

Jet Engine Gas-Path Measurement Filtering Using Center Weighted Idempotent Median Filters

Ranjan Ganguli*
Indian Institute of Science, Bangalore 560 012, India

Key indicators of jet engine health are deviations in gas-path sensor measurements from a "good" baseline engine. These measurement deviations or deltas are used to detect and estimate engine deterioration and faults. Typical measurements are exhaust gas temperature, low rotor speed, high rotor speed, and fuel flow. The measurement deltas are displayed to powerplant engineers through computer visualization tools such as trend plots, which are then used for diagnostic and prognostic decisions. The measurement deltas are also used in pattern recognition and state estimation algorithms to detect and isolate faults. Both the fault detection and the visualization process are hindered by the presence of noise in the data. Traditional linear filters used by the gas turbine industry for smoothing gas-path measurement deltas tend to smooth out the trend shifts in the signal that can signify a fault or repair event. The linear filters also perform poorly when high-amplitude impulsive noise and outliers are present in the signal. However, nonlinear filters can be designed to suppress noise while preserving the final detail in the gas turbine measurements. Results with simulated signals show noise reduction of about 60% can be obtained with a nonlinear center weighted idempotent median filter.

Nomenclature

a	=	smoothing parameter of exponential average filter
b	=	weights of finite impulse response filter
k	=	discrete time
M	=	number of points in sample
N	=	window length of filter
N_1	=	low rotor speed
N_2	=	high rotor speed
W_F	=	fuel flow
w	=	integer median filter weights
x	=	input to filter
y	=	output of filter
z	=	noisy measurement deltas
z^0	=	ideal measurement delta
$\hat{z}$	=	filtered measurement delta
Δ	=	change from baseline "good" engine
η	=	efficiency
Θ	=	root mean square error
θ	=	noise
σ	=	standard deviation, uncertainty
Ψ	=	mathematical representation of filter

Introduction

HEALTH monitoring of jet engines is important because of the high cost of engine failure and the possible loss of human life. Many problems in jet engines manifest themselves as changes in the gas-path measurements.[1–3] Typical gas-path measurements are exhaust gas temperature (EGT), low rotor speed N_1, high rotor speed N_2, and fuel flow W_F. These measurements are also called cockpit parameters because they are displayed to the pilot. Some newer engines also have additional pressure and temperature probes between the compressors and turbines. However, the cockpit parameters are present in both newer and older engines, and therefore, fault detection and isolation systems should be able to work using them to be useful for older engines, which are more susceptible to damage. Jet engine gas-path analysis works on deviations in gas-path measurements from an undamaged baseline engine to detect and isolate faults. These deviations in the measurements from baseline are known as measurement deltas and are plotted vs time. The resulting computer graphics (known as trend plots) are used by powerplant engineers to analyze visually the condition of the engine and its various modules. Unfortunately, noise contaminates the measurements deltas, which can hide key features in the signal from someone observing the data.

A typical measurement delta has two main features. The first is because of long-term deterioration and can be considered to vary in time as a low-degree polynomial, with a very satisfactory linear approximation.[4,5] The second feature of the measurement delta is sudden steplike changes due to so-called single faults. Depold and Gass[6] found from a statistical study of airline data that the main cause of engine in-flight shutdown is single faults, which are preceded by a sharp change in one or more of the measurement deltas. Such a sharp trend change can also occur if the engine is repaired and tested on the ground in a test cell. Therefore, a typical jet engine measurement delta signal can be assumed to be a linear long-term deterioration along with sudden step changes due to a single fault or a repair event.

The powerplant engineer does not only rely on observing trend plots to monitor the engine condition. Various diagnostic algorithms have been developed to estimate engine condition and to identify faults from the health signals using weighted least squares,[7,8] Kalman filter (see Ref. 9), neural network,[6,10–12] fuzzy logic,[13] and Bayesian (see Ref. 14) approaches. However, whereas all of these algorithms attempt to handle the uncertainty in the measurement deltas, their performance is often degraded as the noise in the data increases. This is also true for system identification of jet engines[15] that is done to produce better control and diagnostics models. In addition, these estimation and pattern recognition algorithms are often optimal for Gaussian noise models and can degrade when non-Gaussian outliers are present in the data.[16]

Classical signal processing has been dominated by the assumption of Gaussian random noise model for defining the statistical properties of a real process.[16] However, many real-world processes are characterized by impulsive noise that causes sharp spikes and outliers in the data. For example, data can be corrupted by impulsive noise during acquisition and transmission through communication channels.[17] A phenomenon such as atmospheric noise is also impulsive in nature.[16] Fault detection and isolation methods that are

Received 3 June 2002; revision received 9 April 2003; accepted for publication 29 April 2003.

*Assistant Professor, Department of Aerospace Engineering. Senior Member AIAA.

optimized for random Gaussian noise can suffer severe performance degradation under non-Gaussian noise.

In signal processing, filtering methods are used to preprocess the data to reduce noise. The term noise here is used in a general sense and includes any corruption to the signal that hinders the pattern recognition or state estimation process or that leads to false artifacts being observed during visualization. Traditionally, smoothing methods used by the gas turbine industry are moving averages and exponential smoothing.[6] The moving average is a special case of the finite impulse response (FIR) filter and the exponential average is a special case of the infinite impulse response (IIR) filter. Depold and Gass[6] first addressed the problem of finding a filter that preserves the sharp trend shifts in gas-path measurements due to a single fault. They showed that the exponential average filter has faster reaction time than the widely used 10-point average and is, therefore, a better filtering method for processing data before trend detection and fault isolation. They also developed some rules of thumb to remove outliers from gas turbine measurements. These rules were based on the logic that a shift in any one measurement without shifts in the other measurements would indicate an outlier.

However, both the FIR and IIR filters are linear filters and remove noise while blurring the edges in the signal. In addition, the human visual system is acutely sensitive to high frequency in the spatial form of edges.[18] Most of the low frequency in an image is discarded by the visual system before it can even leave the retina. Unfortunately, the presence of sporadic high-amplitude impulsive noise in a signal can confuse the human visual system into seeing "patterns" where none are really present. Such noise can also trigger an automated trend detection system to give a false alarm. Therefore, it is necessary to remove any such high-amplitude noise while preserving edges from the measurement deltas before subsequent data processing operations for fault detection and isolation.

Substantial research efforts have been conducted in the field of image processing to find suitable alternatives to linear filters that are robust or resistant to the presence of impulsive noise. Among these works, the approach that has received the most attention is that of median filters. Median filters are a well-known and useful class of nonlinear filters in the image processing field.[19–24] They are useful for removing noise while preserving fine details in the signal. However, they are not well known in engineering health monitoring applications. Ganguli[25] used FIR median hybrid (FMH) filters[20] for removing noise from gas turbine measurements while preserving trend shifts. In this study, step changes were considered in a constant signal as a representation of a single fault event. Results showed that the FMH filter preserved the sharp trend shifts in the signal, whereas the moving-average and exponential-average filter smoothed the trend shifts. The problem of deterioration was not addressed. Furthermore, the FMH filter used in this study required up to 10 points of forward data, and therefore, had a 10-point time lag. Because jet engines often get only 1 or 2 points in each flight, the 10-point time lag is very large and is more suitable for engines with online diagnostics systems or for systems where data are obtained rapidly. The cost of high rate data acquisition remains quite high. In applications other than gas turbine engines, Nounou and Bakshi[26] used the FMH filter to remove noise from chemical process signals. Manders et al.[27] used a median filter of length five to remove noise in temperature data for monitoring the cooling system of an automobile engine with installed thermocouples and pressure sensors. Ogaja et al.[28] used FMH filters to remove noise from data measured by a global positioning system (GPS) that directly measures relative displacement and position coordinates for a tall building.

Nonlinear filters are not limited to median type filters. A special neural network called the autoassociative neural network (AAAN)[29,30] has been used for noise filtering, sensor replacement and gross error detection and identification. Lu et al.[11] and Lu and Hsu[31] recently used autoassociative neural networks for noise filtering gas path measurements. The AAAN performs a unitary mapping, which maps the input parameters onto themselves. The AAAN is also capable of removing any outliers in the data and performs better at preserving trend shifts than the moving-average or exponential-average filter. To train the AAAN, noisy data are input to it and mapped to noise-free data at the output nodes. The number of input nodes and output nodes are equal to the number of measurements. The AAAN has an input and output layer, two hidden layers, and a bottleneck layer. Thus the data go to the input layer, then a hidden layer, then a bottleneck layer, followed by a hidden layer and the output layer. Lu et al.[11] used 8 measurements nodes for the hidden layer and 5 nodes for the bottleneck layer resulting in an 8–9–5–9–8 AAAN architecture. Therefore, the neural network learns the noise characteristics of the data and is trained to give noise-free data from noisy data.

Many filtering algorithms use a fixed noise detection threshold obtained at a preassumed noise density level. For example, wavelet-based noise removal methods[26,32,33] use orthogonal wavelet analysis, which finds coefficients related to undesired features in the signal. Nounou and Bakshi[26] showed that wavelet-based noise removal methods could be superior to the FMH filter for process signals with sharp trend shifts. The wavelet-based noise removal has three parts: 1) orthogonal wavelet transform, 2) thresholding of wavelet coefficients, and 3) inverse wavelet transform. When the wavelet coefficients at the highest orthogonal level of decomposition are set to zero, noise can be removed from the signal. However, finding a threshold depends on the noise level and nature of the noise and is a difficult problem. Neural-network-based filtering methods are also sensitive to the noise levels in the training data. For example, the AAAN used by Lu et al.[11] was trained with representative noisy date using simulated signals. However, when the noise characteristics becomes different from that used in algorithm development, which can happen in practical applications, the performance of these algorithms can show degradation.

In this paper, we use a special type of median filter called the center weighted idempotent median (CWIM) filter to process gas turbine health signals for improved visualization and analysis. The filter requires only 2 forward data points compared to 10 points required by the FMH filter. In addition, the filter is demonstrated on signals containing both deterioration and sharp trend shifts. A key advantage of the filters studied in the paper is that they do not need a priori knowledge of the noise characteristics of the signal.

Jet Engine Diagnostics

Figure 1 shows a scheme of the jet engine health monitoring process. The measurement deltas are processed using smoothing algorithms based on moving or exponential averages.[6] In some cases, the health monitoring function may be completely performed by powerplant engineers. In these cases, the measurement deltas are visualized using computer graphics, and the powerplant engineer uses previous experience to detect engine deterioration or faults. In case a fault or severe performance degradation is detected, the powerplant engineer may suggest prognostics and maintenance action. In other cases, the powerplant engineer may also have access to automated fault detection and isolation software that can estimate the condition of the different modules and also detect and isolate other faults. In addition, expert systems may be available for interpreting the output of the fault detection and isolation algorithms for suggesting maintenance and prognostics action. In general, both the automated and human components of the diagnostics system should be used for the best possible decisions.

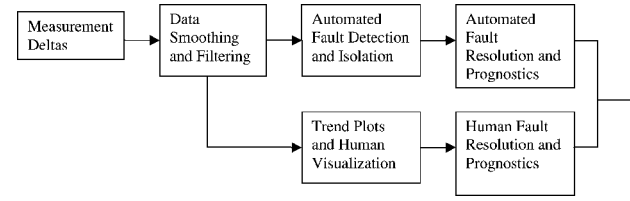

Fig. 1 Scheme of jet engine diagnostics process.

Note from Fig. 1 that a key component of the diagnostics system is the smoothing or filtering function. Although much research has been conducted on the fault detection and isolation function, not much work has been done to improve the data smoothing and filtering function.[6,11,25,31] The next two sections give a brief background on linear filters and the nonlinear median filter.

Linear Filters

The FIR filter can be represented as

$$y(k) = \sum_{i=1}^{N} b(i)x(k-i+1) \tag{1}$$

where $x(k)$ is the kth input measurement and $y(k)$ is the kth output. N is the filter length and $\{b(i)\}$ is the sequence of weighting coefficients that define the characteristics of the filter and sum to unity. When all of the weights $\{b(i)\}$ are equal, the FIR filter reduces to the special case of the mean or average filter, which is widely used for data smoothing. For example, the 10-point moving average has the form

$$y(k) = (1/10)[x(k) + x(k-1) + x(k-2) + \cdots + x(k-9)] \tag{2}$$

Each of the 10 weights for this filter is equal to 1/10.

IIR filters are linear filters with infinite filter length. Exponentially weighted moving average is a popular IIR filter that smoothes a measured data point $x(k)$ by exponentially averaging it with all previous measurements $y(k-1)$:

$$y(k) = ax(k) + (1-a)y(k-1) \tag{3}$$

The parameter a is an adjustable smoothing parameter between 0 and 1 with values such as 0.15 and 0.25 being routinely used in applications.[6] The exponential-average filter has memory because it retains the entire time history by using the output of the last point. Further details about linear filters are available from textbooks.[34]

Median Filters

Nonlinear median filters are discussed next, from the basic standard median filter to the more powerful weighted median filter, center weighted median filter, and idempotent median filters.

Standard Median Filters

Standard median (SM) filters are a popular and useful class of nonlinear filters. The success of median filters is based on two properties: edge preservation and noise reduction with robustness against impulsive type noise. Neither property can be achieved by traditional linear filtering without using time consuming and often ad hoc data manipulation. The median filter with length or window of $N = 2K + 1$ can be represented as[19]

$$y(k) = \text{median}[x(k-K), x(k-K+1), \ldots, x(k), \ldots, x(k+K-1), x(k+K)] \tag{4}$$

where $x(k)$ and $y(k)$ are the kth sample of the input and output sequences, respectively. To compute the output of a median filter, an odd number of sample values are sorted, and the median value is used as the filter output. Thus, the median filter uses both past and future values of $x(k)$ for predicting the current output point. This filter for discrete time k and window length $N = 2K + 1$ can be written in compact form as

$$y = \text{median}(x_{-k}, \ldots, x_{-1}, x_0, x_1, \ldots, x_k) \tag{5}$$

Because the output of a median filter is always one of the input samples, it is possible that certain signals can pass through the median filter without being unaltered. This has been shown to hold for median and many median-based filters. Because such signals define the nature of a filter, these are referred to as root signals. A root is a signal that is not modified by further filtering. Thus, a signal is a root signal of the SM filter if it satisfies

$$x_0 = \text{median}(x_{-k}, \ldots, x_{-1}, x_0, x_1, \ldots, x_k) \tag{6}$$

Repeated median filtering of any finite length signal will result in a root signal after a finite number of passes. It has been shown that if an SM filter has filter window width $2K + 1$ and the signal has length P, then at most

$$3\left[\frac{P-2}{2(K+2)}\right]$$

passes of the filter are required to produce a root signal.[35] However, this bound is rather conservative in practice. Typically, after 5–10 filterings only slight, if any, changes take place in the filter output, and the filter is said to have converged.

It is important to determine if a filter will drive any input signal to one of these roots after a sufficient but finite number of passes. If it does, the filter is said to have convergence property. The important fact is the step edges, ramp edges of sufficient extent, and constant regions are root signals of the median filter. This means that such signals are preserved even after repeated filtering, which is very important to the feature preservation property of the median-type filters.

Weighted Median Filter

The weighted median (WM) filter is a generalization of the SM filter where nonnegative integer weights are assigned to each position in the filter window. WM filters provide a number of free parameters in the form of weights that can be tuned to design a filter to perform specific tasks. WM filters have been successfully used in image processing where edges are very important details. The WM filter output is given as[19]

$$y(k) = \text{median}[w(k-K) \circ x(k-K), \ldots, w(k) \circ x(k), \ldots, w(k+K) \circ x(k+K)] \tag{7}$$

where $\circ$ stands for duplication. Duplication means that the sample $x(k)$ is repeated $w(k)$ times in the array before taking the median. There are $N = 2K + 1$ weights for the WM filter. If we assume that Eq. (7) is defined for the kth sample, we can write the definition of the WM filter in more compact form as

$$y = \text{median}(w_{-k} \circ x_{-k}, \ldots, w_{-1} \circ x_{-1}, w_0 \circ x_0, w_1 \circ x_1, \ldots, w_k \circ x_k) \tag{8}$$

Symmetric WM filters are widely used in practice to avoid bias effects. A symmetric WM filter has weights satisfying the relationship $w_{-1} = w_i$, $i = 1, 2, \ldots, K$.

Note that WM filters with positive integer weights are limited to low-pass capabilities. Low-pass filters remove high-frequency noise. Arce[36] generalized the weights to negative weights by using the following definition:

$$y = \text{median}[|w_{-k}| \circ \text{sgn}(w_{-k})x_{-k}, \ldots, |w_{-1}| \circ \text{sgn}(w_{-1})x_{-1}, |w_0| \circ \text{sgn}(w_0)x_0, |w_1| \circ \text{sgn}(w_1)x_1, \ldots, |w_k| \circ \text{sgn}(w_k)x_k] \tag{9}$$

Here the weight signs are uncoupled with the weight magnitudes and merged with observation samples. This extension to negative weights allows the use of a WM filter to do bandpass or high-pass filtering and to suppress desired frequencies, respectively. The weights of the filter could be optimized for specialized application.[36] However, in our application, we are looking for a low-pass filter contaminated with high-frequency Gaussian noise. Hence, we consider positive integer weights only.

Center Weighted Median Filter

A subclass of the symmetric weighted median filter is the center weighted median (CWM) filter.[22–24] In the CWM filter, all samples inside the filter window are assigned unit weights except the center sample. Thus, a CWM filter with window size $2K + 1$ has a weight

of $w_0 = 2L + 1$ for the center sample, and all other weights are $w_i = 1$ for each $i \neq 0$, where L and K are nonnegative integers,

$$y = \text{median}(x_{-k}, \ldots, x_{-1}, 2L + 1 \circ x_0, x_1, \ldots, x_k) \qquad (10)$$

Different CWM filters are produced by different values of L. When $L = 0$, the CWM filter reduces to the SM filter. When $L \geq K$, the CWM becomes the identity filter because the number of duplications of the center sample results in the median becoming equal to the center sample. Root structures for the CWM filter have the following theorems.

Theorem 1. The minimum length of a constant neighborhood of CWM of window length $2K + 1$ and center weight $2L + 1$ is $K + 1 - L$.

Theorem 2. An edge is a root of any CWM filter.

Proofs of these theorems may be found in Ref. 22.

CWIM Filter

When $L = K - 1$, the CWM filter is an idempotent filter,[37] that produces root signals after a single filtering pass. This avoids the need for repeated passes that are needed by other types of median-based filters to converge to the root signal. Thus, a CWIM filter of window length $2K + 1$ can be defined as

$$y = \text{median}(x_{-k}, \ldots, x_{-1}, 2K - 1 \circ x_0, x_1, \ldots, x_k) \qquad (11)$$

Filter Design for Gas-Path Measurements

The approach of designing a filter to preserve certain image details while discarding others is known as optimal filtering under structural constraints.[22] The CWM filter has two design parameters that must be determined to meet certain requirements. These are the center weight $2L + 1$ and the window length $2K + 1$. A typical design objective is to find a CWM filter to preserve certain signal structures, for example, the smallest length constant neighborhood that is a set of adjacent points having similar values.

Using Theorems 1 and 2, we could design a filter for specific applications. For jet engine measurement deltas, we can assume that any one point that is not a part of a trend or constant neighborhood is a spurious data point representing impulsive noise. However, any two or more points that represent a trend are assumed to reflect a genuine trend. This is a very conservative assumption and ensures that any fine details in the image lasting over one point are preserved. We want a filter with minimum need for forward data. This can be accomplished by using a filter of small window length (for example, a three-point filter). However, larger window lengths lead to better noise attenuation. As a compromise, we select a five-point filter with window length $N = 2K + 1 = 5$. This results in $K = 2$ and a time delay of only two data points in the signal.

From Theorem 1, we see that the minimum length of a constant neighborhood of CWM of window length $2K + 1$ and center weight $2L + 1$ is $K + 1 - L$. Therefore, for preserving constant neighborhoods of minimum length 2, we need $K + 1 - L = 2$; this yields $L = 1$. The center weight is then equal to $2L + 1 = 3$. The corresponding filter with $K = 2$ and $L = 1$ is

$$y = \text{median}(x_{-2}, x_{-1}, 3 \circ x_0, x_1, x_2) \qquad (12)$$

The preceding filter is also an idempotent filter because $L = K + 1$. Therefore, it should converge to a root signal in only one pass and not need repeated passes like the conventional median filters. We shall use this five-point CWIM filter with triple duplication of the center sample for our results. The filter preserves constant neighborhoods of minimum length equal to 2 and does not preserve constant neighborhoods of length less than 2. From Theorem 2, an edge is always preserved by the CWM filter. Therefore, it preserves fine details but removes spurious impulsive noise.

Test Signal

Gas-path measurement deltas are obtained by subtracting the baseline measurements for a good engine from the actual measurements. The baseline measurements often come from an engine model, and various correction factors are used to reduce the measured data to standard sea-level conditions.[38] Because both the engine model and the correction factors are mathematical model idealizations, they are sources of errors in the gas-path measurements deltas. Therefore, gas-path measurement deltas contain high levels of uncertainty due to sensor errors and modeling approximations.

Table 1 Fingerprints for selected gas turbine faults for $\eta = -2\%$

Faults	Δ EGT, °C	ΔW_F, %	ΔN_2, %	ΔN_1, %
HPC	13.60	1.60	−0.11	0.10
HPT	21.77	2.58	−1.13	0.15
LPC	9.09	1.32	0.57	0.28
LPT	2.38	−1.92	1.27	−1.96
Fan	−7.72	−1.40	−0.59	1.35

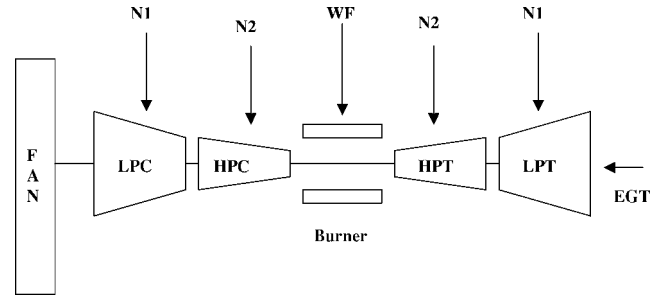

Fig. 2 Scheme of jet engine modules and sensor measurements.

A typical twin spool jet engine (Fig. 2) consists of five modules: fan, low-pressure compressor (LPC), high-pressure compressor (HPC), high-pressure turbine (HPT), and low-pressure turbine (LPT). Air coming into the engine is compressed in the fan, LPC, and HPC modules, combusted in the burner, and then expanded through the LPT and HPT modules, producing power. The sensors N_1, N_2, W_F, and EGT provide information about the condition of these modules and are used for health monitoring. Table 1 shows influence coefficients for a commercial jet engine at a fixed power condition with $\eta = -2\%$ from a baseline good engine. These influence coefficients are taken from Ref. 12. The numbers in Table 1 are the fingerprints or fault signatures for the module faults. As an example, a 2% efficiency decrease in the HPC corresponds to a 13.6°C increase in exhaust gas temperature, a 1.6% increase in the fuel flow, a 0.11% decrease in high rotor speed, and a 0.10% increase in low rotor speed. Test signals are created for the four measurements with the fingerprint chart numbers as a guide for the maximum measurement deltas. Using synthetic test signals allows us to evaluate the filter performance because the final answer is known.

Ideal Signal

The signals in Figs. 3–6 contain 250 data points for the Δ EGT, ΔW_F, ΔN_2, ΔN_1, and measurements, respectively. In Figs. 3–6, an ideal, noisy and CWIM, FIR, and IIR filtered signal is shown. The ideal test signals used in this study are obtained by putting together linear deterioration signals superimposed with edges representing a single fault or maintenance event. A number of combinations of the deterioration and fault signals are studied. This simulated fault time history idealizes a real-life scenario within a compressed timescale. The maximum amplitude values uses for each signal are Δ EGT = 15.4°C, $\Delta W_F = 1.91\%$, $\Delta N_2 = -0.74\%$, and $\Delta N_1 = -1.99\%$, which correspond to, for example, an HPT fault of $\eta = -1.41\%$, an HPT fault of $\eta = -1.48\%$, an HPT fault of $\eta = -1.31$, and an LPT fault of $\eta = -1.97\%$, respectively (from Table 1).

Noisy Signal

Random noise is added to the simulated measurements using standard deviations for Δ EGT, ΔN_1, ΔN_2 and, ΔW_F of 4.23°C, 0.25%, 0.17% and 0.50%, respectively. These numbers are obtained from typical airline data given in Ref. 12. Impulsive noise is also added

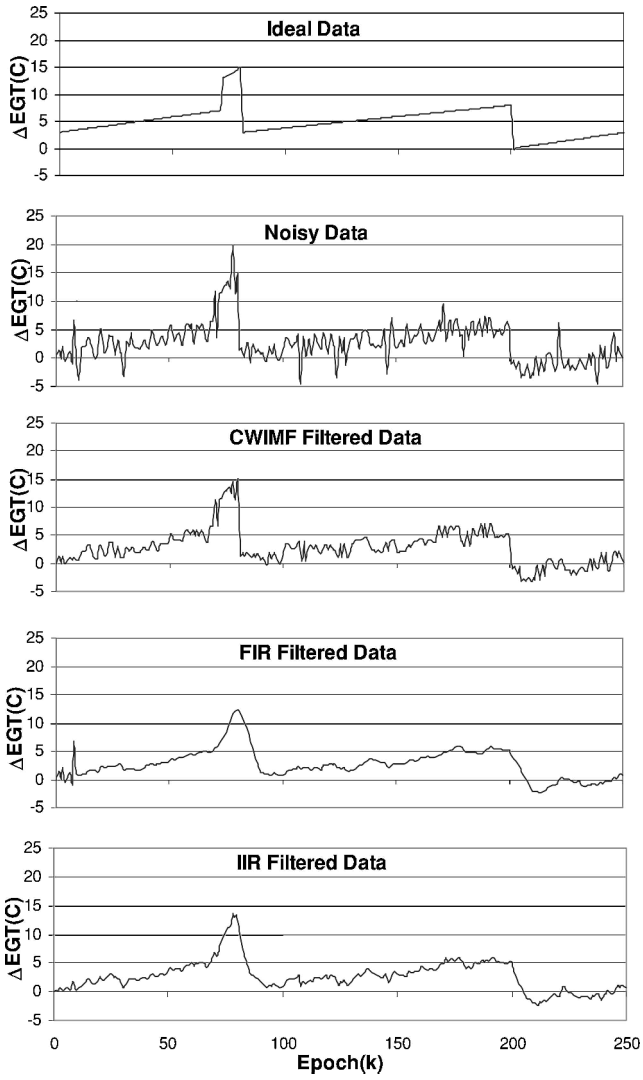

Fig. 3 Ideal, noisy, and filtered Δ EGT data.

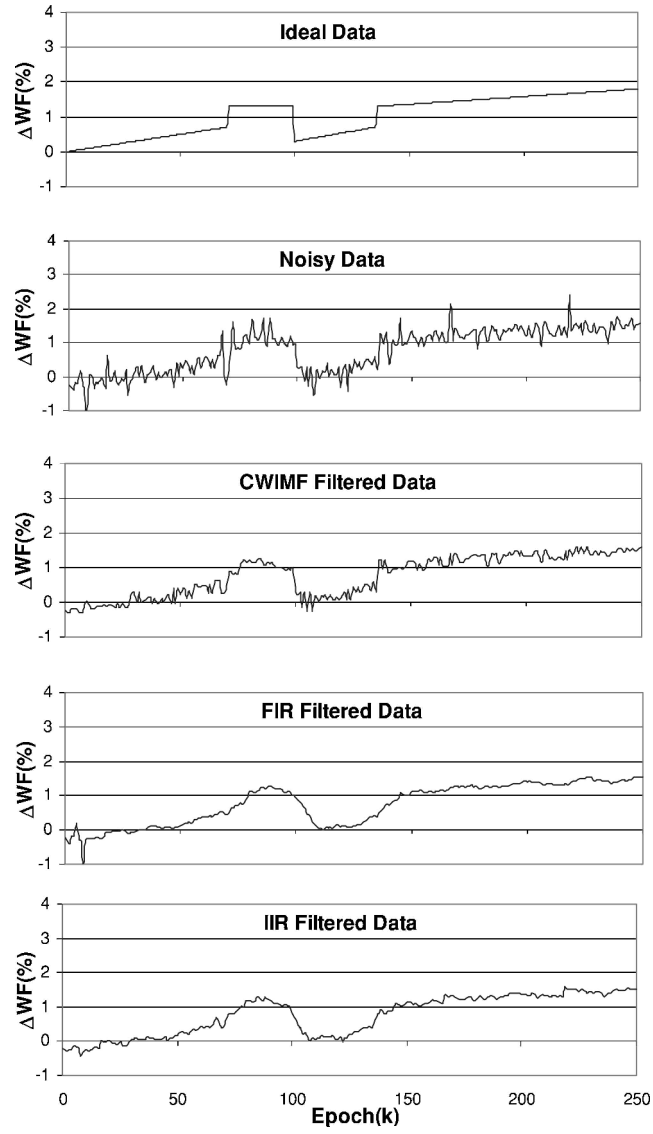

Fig. 4 Ideal, noisy, and filtered ΔW_F data.

to the ideal signal. The impulses are selected at eight levels: σ, 1.5σ, 1.75σ, 2σ, $-\sigma$, -1.5σ, -1.75σ, and -2σ. These points are placed in an arbitrary way to simulate spurious data that follows no theoretical noise model. The noisy signal is shown in Figs. 3–6 for the four measurements. Both random and impulsive noises are included in that signal. Note that noise causes problems in differentiating between a healthy and damaged engine and also hides important features of the data.

After noise is added to this signal, it allows us to test the performance of a filter in the presence of trend shifts that can represent a single fault precursor to a major maintenance event and also ramps, which model long-term deterioration over time. The stationary regions simulate a healthy engine. The test signals used here are relatively more complex than those found in actual practice. However, they serve to illustrate the CWIM, FIR, and IIR filters over a range of signal-to-noise ratios and for different deterioration rates and trend shifts.

Error Measure

Consider the basic measurement deltas Δ EGT, ΔN_1, ΔN_2, and ΔW_F. Then we can write any of these measurement deltas as follows:

$$z = z^0 + \theta \tag{13}$$

where z^0 is the measurement delta also called the ideal signal. In reality such a pure signal would be contaminated by noise and outliers, and therefore, z is the polluted or corrupted signal. A filter Ψ performs the following operation that returns the filtered signal from the corrupted signal:

$$\hat{z} = \Psi(z) = \Psi(z^0 + \theta) \tag{14}$$

In the next section, we evaluate the CWIM, FIR, and IIR filters using simulated data. The following root mean square error measure based on the L_2 norm will be used to analyze the filter performance over a sample of M points by comparing the filtered signal with the ideal signal[39]:

$$\Theta = \frac{1}{M}\sum_{k=1}^{M}\sqrt{\left(\hat{z}_k - z_k^0\right)^2} \tag{15}$$

Numerical Experiments

Numerical experiments are conducted to evaluate qualitatively and quantitatively the CWIM filter and the traditional linear filters using the test signals. Figures 3–6 show the ideal, noisy and filtered signals for Δ EGT, ΔW_F, ΔN_2, and ΔN_1, respectively. It is verified that the ideal signal for each of the four cases are indeed root signals of the CWIM filter. This is not surprising because constant regions, step edges, and ramp edges of sufficient extent are root signals of median filters, as mentioned by Senel et al.[21] The FIR filter used in Figs. 3–6 uses a 10-point moving average [Eq. (2)] and the IIR filter uses $a = 0.25$ in Eq. (3).

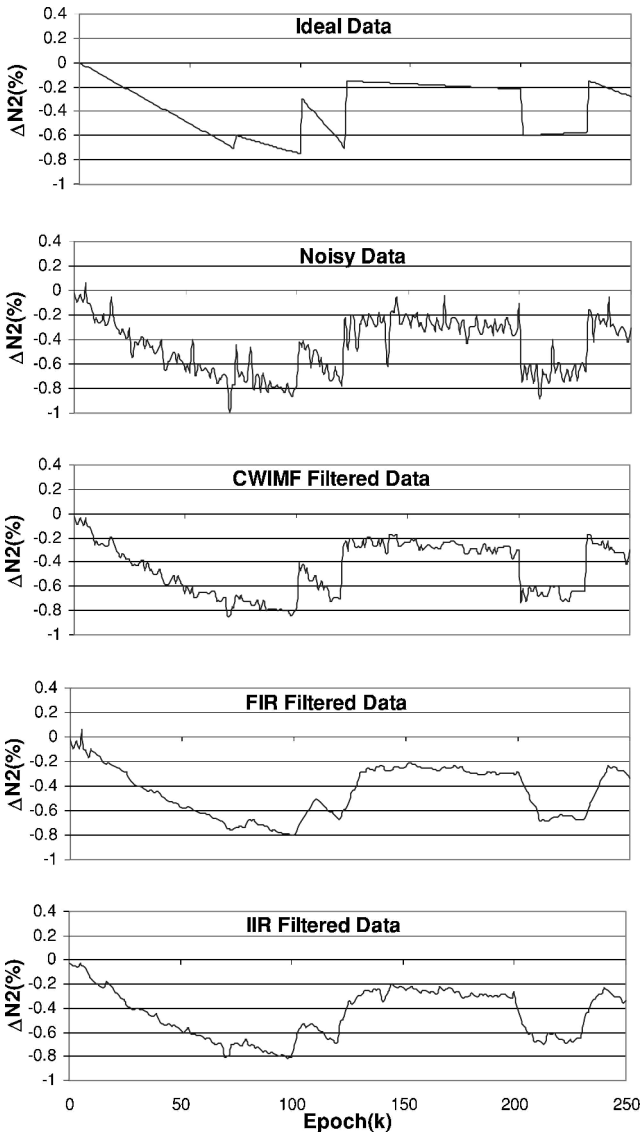

Fig. 5 Ideal, noisy, and filtered ΔN_2 data.

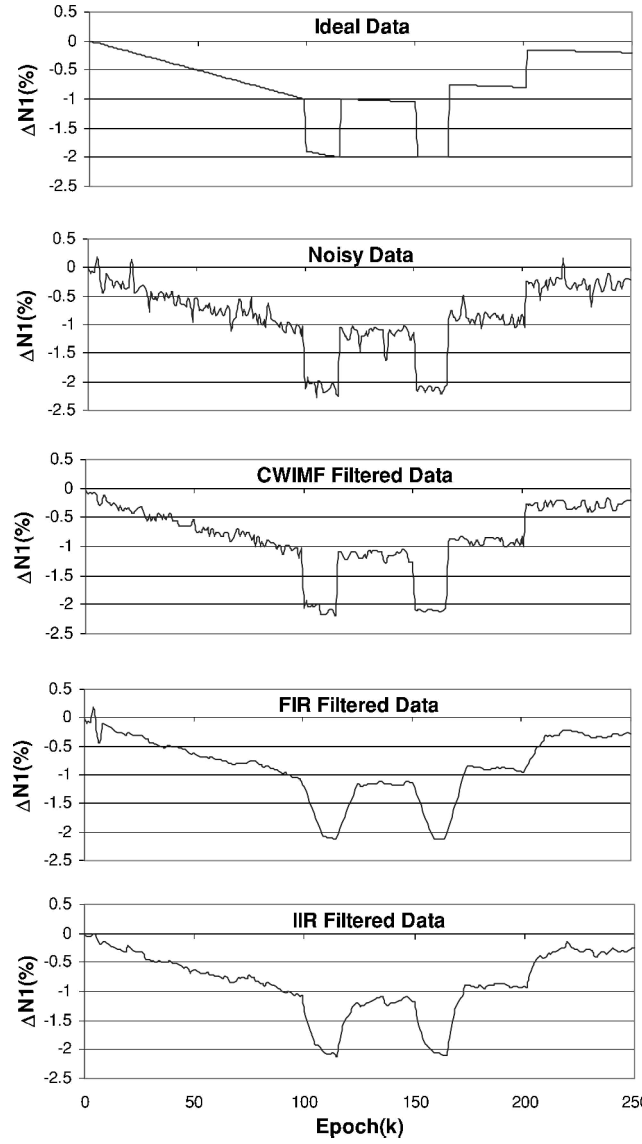

Fig. 6 Ideal, noisy, and filtered ΔN_1 data.

Observe from Figs. 3–6 that considerable noise is reduced for each signal after CWIM filtering and that trend changes and deterioration history are more clearly visible. For the Δ EGT signal in Fig. 3, the three points where trend shifts occur are clearly identified. In addition, the linear variations simulating engine deterioration are also preserved. The impulsive outliers in the data are successfully removed. The FIR filter is very good at removing the high-frequency random noise and absorbing the outliers. However, the FIR filter smoothes out the trend shifts. The FIR filter also takes nine points to start, which results in some impulsive noise in the signal between $k = 1$ and $k = 9$ not being smoothed. In contrast, the IIR filter needs one point to start and the CWIM filter needs two points. The IIR filter also reduces random noise, but smoothes out the trend shifts in the signal. For the ΔW_F signal in Fig. 4, the three points where the trend shifts occur are clearly identified after CWIM filtering. The linear characteristics in the signal are also preserved. For the ΔN_2 signal in Fig. 5, the step edges are clearly preserved, and their temporal locations are enhanced in the signal after CWIM filters. In addition, the fine detail due to a small trend shift between $k = 50$ and $k = 100$ is also brought out in the filtered signal. Such fine detail is very difficult to decipher in the noisy signal. Finally, the ΔN_1 signal in Fig. 6 shows the step edges and deterioration features are clearly brought out.

The results also show that the CWIM filter works best in removing outliers and not in removing Gaussian noise. Thus, for the Δ EGT and ΔW_F signals, which have high levels of Gaussian noise, the CWIM filtered signal still contains more random noise that the FIR and IIR filtered signals. For the ΔN_2 and ΔN_1 signals, which have low random noise levels, the filtered signal appears much less noisy. This is not surprising because the CWIM filter used here falls under the class of the "gentle filter," which removes outliers while to a large extent not affecting other features.[19] In contrast, the FIR and IIR filters remove Gaussian noise. However, fault isolation algorithms such as the Kalman filter, which is used for gas-path state estimation, are only optimal under a Gaussian noise environment.[40] Therefore, such algorithms can handle the Gaussian noise present in the data, but would have problems with non-Gaussian outliers.

The impulses that corrupted the signal and prevented proper visualization have been removed by the CWIM filter. The removal of impulsive noise is important for improved visualization because the human visual system is very sensitive to high frequency in the form of edges. The removal of the impulsive noise also makes the filtered signal more amenable to automated fault detection and isolation.

The results shown in Figs. 3–6 are qualitative and represent one of many possible noisy samples. For a more quantitative understanding, 1000 samples of noisy random data about the ideal signals shown in Figs. 3–6 were taken for each of the four measurements, and the average root mean square error calculated. These results are shown in Table 2. For each of the four measurements, there is a reduction in noise of about 58–60% for the CWIM filtered signal compared to the noisy signal.

Table 2 Average root mean square error for noisy and CWIM filtered data

Data	Δ EGT	ΔW_F	ΔN_2	ΔN_1
Noisy	0.156	0.0046	0.0062	0.0091
Filtered	0.064	0.0019	0.0025	0.0037

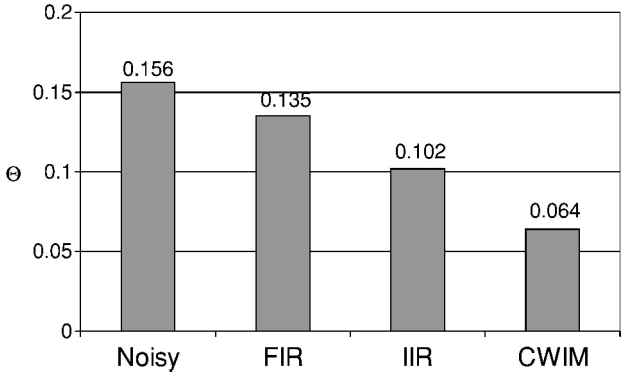

Fig. 7 Average root mean squared error for noisy and FIR, IIR, and CWIM filtered Δ EGT data.

To illustrate the benefit of the CWIM filter over the linear filter, Fig. 7 is a comparison of the noise reduction in Δ EGT using the FIR, IIR, and CWIM filters. Compared to the noisy signal, the FIR filter shows a noise reduction of 13%, the IIR filter of 35%, and the CWIM filter of 59%. Therefore, the nonlinear CWIM filter can be recommended for noise removal from jet engine gas-path measurements.

Conclusions

A nonlinear filter, the CWIM filter, is analyzed for improved visualization and noise removal in jet engine gas-path measurements. A typical jet engine measurement delta signal is created using linear deterioration superimposed with occasional trend shifts. The four measurements considered are exhaust gas temperature, fuel flow, low rotor speed, and high rotor speed. The following conclusions are drawn from this study.

1) A nonlinear CWIM filter is specially designed for noise removal in jet engine measurement signals. This filter results in a noise reduction of about 60% in all four measurements used in this study.

2) The CWIM filter retains the trend shifts and other features in the signal while removing noise. It helps in generating a signal that is more suited to the human visual system by removing high-amplitude impulsive noise that can lead to a person observing patterns where none are really present.

3) Filtering gas-path measurements using the CWIM filter before fault detection and isolation is likely to improve the performance of state estimation algorithms such as the Kalman filter, which are optimal for Gaussian noise and can show performance degradation in the presence of non-Gaussian outliers.

4) The linear FIR and IIR filters typically used for smoothing jet engine signals are found to smooth out the key features in the signal. For the exhaust gas-path temperature signal, the noise reduction by the FIR, IIR, and CWIM filters is 13, 35, and 59%, respectively. Therefore, the CWIM filter is recommended for preprocessing jet engine measurement deltas before performing fault detection or visualization.

References

[1]Sieros, G., Stamasis, K., and Mathioudakis, K., "Jet Engine Component Maps for Performance Modeling and Diagnosis," *Journal of Propulsion and Power*, Vol. 13, No. 5, 1997, pp. 665–674.

[2]Pinelli, M., and Spina, P. R., "Gas Path Field Performance Determination: Sources of Uncertainties," *Journal of Engineering for Gas Turbine and Power*, Vol. 124, No. 1, 2002, pp. 155–160.

[3]Li, Y. G., "Performance Analysis Based Gas Turbine Diagnostics: a Review," *Journal of Power and Energy*, Vol. 216, No. 5, 2002, pp. 363–377.

[4]Fasching, W. A., and Stricklin, R., "CF6 Jet Engine Diagnostics Program: Final Report," NASA CR 165582, 1982.

[5]Mathioudakis, K., Kamboukos, P., and Stamasis, A., "Turbofan Performance Deterioration Tracking Using Non-Linear Models and Optimization Techniques," *Journal of Turbomachinery*, Vol. 124, No. 4, 2002, pp. 580–587.

[6]DePold, H., and Gass, F. D., "The Application of Expert Systems and Neural Networks to Gas Turbine Prognostics and Diagnostics," *Journal of Engineering for Gas Turbine and Power*, Vol. 121, No. 4, 1999, pp. 607–612.

[7]Doel, D. L., "TEMPER—A Gas-Path Analysis Tool for Commercial Jet Engines," *Journal of Engineering for Gas Turbines and Power*, Vol. 116, No. 1, 1994, pp. 82–89.

[8]Doel, D. L., "Interpretation of Weighted Least Squares Gas Path Analysis Results," *47th American Society of Mechanical Engineers, Gas Turbine and Aeroengine Technical Conf.*, June 2002.

[9]Urban, L. A., and Volponi, A. J., "Mathematical Methods of Relative Engine Performance Diagnostics," Society of Automotive Engineers, Paper SAE 922048, 1992.

[10]Zedda, M., and Singh, R., "Neural Network Based Sensor Validation for Gas Turbine Test Bed Analysis," *Journal of Systems and Control in Engineering*, Vol. 215, No. 1, 2000, pp. 47–56.

[11]Lu, P. J., Hsu, T. C., Zhang, M. C., and Zhang, J., "An Evaluation of Engine Fault Diagnostics Using Artificial Neural Networks," *Journal of Engineering for Gas Turbine and Power*, Vol. 123, No. 2, 2001, pp. 240–246.

[12]Volponi, A. J., Depold, H., Ganguli, R., and Daguang, C., "The Use of Kalman Filter Neural Network Methodologies in Gas Turbine Performance Diagnostics: A Comparative Study," American Society of Mechanical Engineers, ASME Paper 00-GT-547, May 2000.

[13]Ganguli, R., "Fuzzy Logic Intelligent System for Gas Turbine Module and System Fault Isolation," *Journal of Propulsion and Power*, Vol. 18, No. 2, 2002, pp. 440–447.

[14]Romessis, C., Stamatis, A., and Mathioudakis, A. K., "Setting up a Belief Network for Turbofan Diagnosis with the Aid of an Engine Performance Model," International Symposium on Air Breathing Engines, ISABE Paper 1032, Sept. 2001.

[15]Sugiyama, N., "System Identification of Jet Engines," *Journal of Engineering for Gas Turbine and Power*, Vol. 122, No. 1, 2000, pp. 19–26.

[16]Kalluri, S., and Arce, G. R., "Adaptive Weighted Myriad Filter Algorithms for Robust Signal Processing in α-Stable Noise Environment," *IEEE Transactions on Signal Processing*, Vol. 46, No. 2, 1998, pp. 322–334.

[17]Windyga, P. S., "Fast Impulsive Noise Removal," *IEEE Transactions on Image Processing*, Vol. 10, No. 2, 2001, pp. 173–179.

[18]Schroeder, W., Martin, K., and Lorensen, B., *The Visualization Toolkit*, Prentice–Hall, Upper Saddle River, NJ, 1998, pp. 432–435.

[19]Yin, L., Yang, M., Gabbouj, M., and Neunou, Y., "Weighted Median Filters: A Tutorial," *IEEE Transaction on Circuits and Systems*, Vol. 40, No. 1, 1996, pp. 147–192.

[20]Heinonen, P., and Neuvo, Y., "FIR-Median Hybrid Filter," *IEEE Transactions on Acoustics, Speech, and Signal Processing*, Vol. 35, No. 6, 1987, pp. 832–838.

[21]Senel, H. G., Peters, A. R., II, and Dawant, B., "Topological Median Filters," *IEEE Transactions on Image Processing*, Vol. 11, No. 2, 2002, pp. 89–104.

[22]Sun, T., Gabbouj, M., and Neunou, Y., "Center Weighted Median Filters: Some Properties and Their Applications in Image Processing," *Signal Processing*, Vol. 35, No. 3, 1994, pp. 213–229.

[23]Chen, T., Ma, K. K., and Chen, L. H., "Tri-State Median Filter for Image Denoising," *IEEE Transactions on Image Processing*, Vol. 8, No. 12, 1999, pp. 1834–1838.

[24]Chen, T., and Wu, R. H., "Adaptive Impulse Detection Using Center Weighted Median Filters," *IEEE Signal Processing Letters*, Vol. 8, No. 1, 2001, pp. 1–3.

[25]Ganguli, R., "Data Rectification and Detection of Trend Shifts in Jet Engine Gas Path Measurements Using Median Filters and Fuzzy Logic," *Journal of Engineering for Gas Turbines and Power*, Vol. 124, No. 4, 2002, pp. 809–816.

[26]Nounou, M. N., and Bakshi, B. R., "On-line Multiscale Filtering of Random and Gross Errors without Process Models," *AIChE Journal*, Vol. 45, No. 5, 1999, pp. 1041–1058.

[27]Manders, E. J., Biswas, G., Mosterman, P. J., Barford, L., and Bennet, J., "Signal Interpretation for Monitoring and Diagnosis, A Cooling System Testbed," *IEEE Transactions on Instrumentation and Measurement*, Vol. 49, No. 3, 2000, pp. 503–508.

[28]Ogaja, O., Wang, J., Rizos, C., and Brownjohn, J., "Multivariate Monitoring of GPS Observations and Auxiliary Multi-Sensor Data," *GPS Solutions*, Vol. 5, No. 4, 2002, pp. 58–69.

[29]Kramer, M. A., "Non-linear Principal Component Analysis Using Autoassociative Networks," *AIChE Journal*, Vol. 37, No. 2, 1991, pp. 233–243.

[30]Kramer, M. A., "Autoassociative Neural Networks," *Computers and Chemical Engineering*, Vol. 16, No. 4, 1992, pp. 313–328.

[31]Lu, P. J., and Hsu, T. C., "Application of Autoassociative Neural Network on Gaspath Sensor Data Validation," *Journal of Propulsion and Power*, Vol. 18, No. 4, 2002, pp. 879–888.

[32]Staszewski, W. J., "Intelligent Signal Processing for Damage Detection in Composite Materials," *Composite Science and Technology*, Vol. 62, Nos. 7–8, 2002, pp. 941–950.

[33]Staszewski, W. J., "Advanced Data Preprocessing for Damage Identification Based on Pattern Recognition," *International Journal of Systems Science*, Vol. 31, No. 11, 2000, pp. 1381–1396.

[34]Hamming, R. W., *Digital Filters*, 3rd ed., Prentice–Hall, Englewood Cliffs, NJ, 1989.

[35]Wendt, P. D., Coyle, E. J., and Gallagher, N. C., Jr., "Some Convergence Properties of Median Filters," *IEEE Transaction on Circuits and Systems*, Vol. CAS-33, March 1986, pp. 276–286.

[36]Arce, G. R., "A General Weighted Median Filter Structure Admitting Negative Weights," *IEEE Transactions on Signal Processing*, Vol. 46, No. 12, 1998, pp. 3195–3205.

[37]Haavista, P., Juhola, J., and Neunou, Y., "Median Based Idempotent Filters," *Journal of Circuits Systems and Computers*, Vol. 1, No. 2, 1991, pp. 125–148.

[38]Volponi, A. J., "Gas Turbine Parameter Corrections," *Journal of Engineering for Gas Turbines and Power*, Vol. 121, No. 4, 1999, pp. 613–621.

[39]Vardavoulia, M. I., "A New Vector Median Filter for Color Image Processing," *Pattern Recognition Letters*, Vol. 22, Nos. 6–7, 2001, pp. 675–689.

[40]Wu, W. R., and Kundu, A., "Recursive Filtering with Non-Gaussian Noises," *IEEE Transactions on Signal Processing*, Vol. 44, No. 6, 1996, pp. 1454–1468.